J Neurophysiol 98: 952–965, 2007.
First published June 20, 2007; doi:10.1152/jn.00060.2007.

Muscarinic M_2 and M_1 Receptors Reduce GABA Release by Ca^{2+} Channel Modulation Through Activation of PI_3K/Ca^{2+}-Independent and PLC/Ca^{2+}-Dependent PKC

H. Salgado,[1,*] T. Bellay,[1,*] J. A. Nichols,[1] M. Bose,[1] L. Martinolich,[1] L. Perrotti,[2] and M. Atzori[1]

[1]*Laboratory of Synaptic and Cell Physiology, School of Behavioral and Brain Sciences, The University of Texas at Dallas, Richardson Texas; and* [2]*Department of Psychology, University of Texas at Arlington, Arlington, Texas*

Submitted 17 January 2007; accepted in final form 15 June 2007

Salgado H, Bellay T, Nichols JA, Bose M, Martinolich L, Perrotti L, Atzori M. Muscarinic M_2 and M_1 receptors reduce GABA release by Ca^{2+} channel modulation through activation of PI_3K/Ca^{2+}-independent and PLC/Ca^{2+}-dependent PKC. *J Neurophysiol* 98: 952–965, 2007. First published June 20, 2007; doi:10.1152/jn.00060.2007. We measured pharmacologically isolated GABAergic currents from layer II/III neurons of the rat auditory cortex using patch-clamp recording. Activation of muscarinic receptors by muscarine (1 μM) or oxotremorine (10 μM) decreased the amplitude of electrically evoked inhibitory postsynaptic currents to about one third of their control value. Neither miniature nor exogenously evoked GABAergic currents were altered by the presence of muscarinic agonists, indicating that the effect was spike-dependent and not mediated postsynaptically. The presence of the N- or P/Q-type Ca^{2+} channel blockers ω-conotoxin GVIA (1 μM) or ω-AgaTx TK (200 nM) greatly blocked the muscarinic effect, suggesting that Ca^{2+}-channels were target of the muscarinic modulation. The presence of the muscarinic M_2 receptor (M_2R) antagonists methoctramine (5 μM) or AF-DX 116 (1 μM) blocked most of the muscarinic evoked inhibitory postsynaptic current (eIPSC) reduction, indicating that M_2Rs were responsible for the effect, whereas the remaining component of the depression displayed M_1R-like sensitivity. Tissue preincubation with the specific blockers of phosphatidyl-inositol-3-kinase (PI_3K) wortmannin (200 nM), LY294002 (1 μM), or with the Ca^{2+}-dependent PKC inhibitor Gö 6976 (200 nM) greatly impaired the muscarinic decrease of the eIPSC amplitude, whereas the remaining component was sensitive to preincubation in the phospholipase C blocker U73122 (10 μM). We conclude that acetylcholine release enhances the excitability of the auditory cortex by decreasing the release of GABA by inhibiting axonal V-dependent Ca^{2+} channels, mostly through activation of presynaptic $M_2Rs/PI_3K/Ca^{2+}$-independent PKC pathway and—to a smaller extent—by the activation of M_1/PLC/Ca^{2+}-dependent PKC.

INTRODUCTION

Acetylcholine is released by a nonsynaptic network of axon terminals originating from the nucleus basalis of Meynert (NB) into the neocortex where it regulates attention (Passetti et al. 2000; Voytko et al. 1994), cortical rhythms (Buhl et al. 1998; Podol'skii et al. 2000), and plasticity (Kilgard and Merzenich 1998). The attentional control of cortical acetylcholine release is supposed to be regulated by a bi-directional prefrontal cortex (PFC)–NB circuit, whose activation, in turn, induces acetylcholine release on more posterior cortical areas (Sarter et al. 2005a). Impairment of the regulation of cortical cholinergic function is associated with, and at least in part responsible for, the occurrence of Alzheimer disease (cholinergic deficit) and schizophrenia (cholinergic excess, Sarter et al. 2005a,b).

Activation of the virtually ubiquitous muscarinic acetylcholine receptors (Mash and Potter 1986) on GABA–containing (GABAergic) interneurons controls many functions including burst synchronization (Kondo and Kawaguchi 2001), information flow across cortical layers (Xiang et al. 1998), sensory receptive fields (Restuccia et al. 2003), and γ-oscillations generation (Fisahn et al. 1998), prompting at GABAergic interneurons as an exquisitely sensitive target for cholinergic control of neocortical function.

The auditory cortex is subject to strong cholinergic modulation (Aramakis et al. 1997; Hsieh et al. 2000; Kilgard and Merzenich 1998; McKenna et al. 1988; Metherate and Ashe 1991), contributing to processing and storage of auditory information with a variety of cellular mechanisms. Previous studies reported that activation of muscarinic receptors, along with other cellular actions, decreases GABAergic synaptic currents in the auditory cortex (Metherate and Ashe 1995). Limited information is available on the cellular mechanisms and physiological significance of the cholinergic decrease of the GABAergic synaptic activity, representing a crucial component of the physiological and pathological increase in excitability of the auditory neocortex.

In this work, we quantified the cellular and pharmacological characteristics of the muscarinic modulation of GABAergic currents within the first cortico-cortical relay, constituted by the cells of layer II/III of the auditory cortex. We found that activation of muscarinic receptors reduces the release of GABA in the auditory cortex to approximately one third by inhibiting presynaptic voltage-gated Ca^{2+} channels mainly through two pathways: the PI_3K/Ca^{2+}-independent PKC-mediated pathway and the PLC/Ca^{2+}-dependent PKC-mediated pathway. The resulting decrease in GABAergic function has the potential to shift between cortical states by drastically changing neocortical excitability using previously unknown synaptic mechanisms.

METHODS

Preparation

We used an auditory cortex slice preparation similar to one previously described (Atzori et al. 2001). Twenty-three to 40-day-old

* H. Salgado and T. Bellay contributed equally to this study.

Address for reprint requests and other correspondence: M. Atzori, LCSP, SBBS, Univ. of Texas at Dallas, 2601 N. Floyd Rd., Richardson TX 75080.

The costs of publication of this article were defrayed in part by the payment of page charges. The article must therefore be hereby marked "*advertisement*" in accordance with 18 U.S.C. Section 1734 solely to indicate this fact.

Sprague-Dawley rats (Charles River, Wilmington, MA) were anesthetized with isoflurane (Baxter, Round Lake, IL) and killed according to the National Institutes of Health guidelines (UTD IACUC number 04-04), and their brains were sliced with a vibratome (VT1000, Leica) in a refrigerated solution (0–4°C) containing (mM) 130 NaCl, 3.5 KCl, 10 glucose, 24 $NaHCO_3$, 1.25 NaH_2PO_4, 1.5 $CaCl_2$, and 1.5 $MgCl_2$, saturated with a mixture of 95% O_2-5% CO_2 (ACSF). Two hundred seventy-micrometer-thick coronal slices from the most caudal fourth of the brain were retained after removing the occipital convexity and subsequently incubated in ACSF at 32°C before being placed in the recording chamber. The recording area was selected dorsally to the sylvian sulcus corresponding to the auditory cortex (Rutkowski et al. 2003). The recording solution also contained 6,7-dinitroquinoxaline-2,3-dione (DNQX, 10 μM) and kynurenate (2 mM) for blocking α-amino-3-hydroxy-5-methyl-4-isoxazolepropionic acid receptor (AMPAR)– and *N*-methyl-D-aspartate receptor (NMDAR)–mediated currents, respectively.

Drugs and solutions

All drugs were purchased from Sigma (St. Louis, MO), TOCRIS (Ellisville, MO), Peptides International (Louisville, KY), or Alomone Laboratories (Jerusalem, Israel). The muscarinic toxin MT1 was a generous gift from Alomone Laboratories. In some experiments, pulses of the $GABA_A$ agonist muscimol (100 μM) were applied at 100–200 μm from the recording areas, once every 30 s. A stock solution of muscimol was diluted 10-fold in ACSF before being back-filled to a glass pipette similar to the one used for recording. Muscimol application was performed using a pressure system (picospritzer, General Valve, Fairfield, NJ) through a glass pipette ($\cong$25 psi, 3–12 ms). Stock solutions of all drugs were prepared in water except for U73122, AF-DX 116, and bisindolymaleimide, whose stock solutions were prepared in dimethylsulfoxide (final concentration, 0.1%). For nonaqueous solutions, the final concentration of the solvent was added to the recording control solution. Drugs were bath-applied into the recording chamber except for U73122, pertussis toxin (PTX), wortmannin, LY-294002, bisindolymaleimide, and Go6976, which were added to the incubation chamber as a pretreatment as specified in the text. PTX was activated according to Kaslow et al. (1987). After recording an initial baseline for 7–10 min, drugs were bath-applied for 5 min or longer, until reaching a stable condition (see *Statistical analysis*).

Electrophysiology

Slices were placed in an immersion chamber, where cells with a prominent apical dendrite, suggestive of pyramidal morphology, were visually selected using a BX 51 (Olympus) with an infrared camera system (DAGE-MTI, Michigan City, IN). Inhibitory postsynaptic currents (IPSCs) were recorded in the whole cell configuration, in voltage-clamp mode, holding the membrane potential at $V_h = -60$ mV, with 3–5 MΩ electrodes filled with a solution containing (mM) 100 CsCl, 5 1,2-bis(2-aminophenoxy)ethane-*N,N,N′,N′*-tetraacetic acid K (BAPTA-K), 1 lidocaine *N*-ethyl bromide (QX314), 1 $MgCl_2$, 10 HEPES, 4 glutathione, 1.5 $ATPMg_2$, 0.3 $GTPNa_2$, 8 biocytin, and 20 phosphocreatine. The intracellular recording solution was titrated at pH 7.3 and had an osmolarity of 270 mOsm. The holding voltage was not corrected for the junction potential (<4 mV). Electrically evoked IPSCs (eIPSCs) were measured by delivering two electric stimuli (90–180 μs, 10–50 μA) 50 ms apart every 20 s with an isolation unit, through a glass stimulation monopolar electrode filled with ACSF, and placed at ~150–200 μm from the recording electrode. A 2-mV voltage step was applied at the beginning of every episode to monitor the quality of the recording. In the analysis of miniature postsynaptic currents, only well-isolated minis were considered for kinetic analysis. All events that satisfied a preset criterion, analyzed with Clampfit software (Axon, Burlingame, CA), were considered in the calculation of the event frequency. The average number of events per each condition was >300.

Biocytin injections

All recorded neurons were injected with 8 mM biocytin in the intracellular solution. After all recordings, slices were immediately transferred to a 24-well plate and fixed in a solution containing 80 mM Na_2HPO_4, 80 mM NaH_2PO_4, and 4% paraformaldehyde. Biocytin staining was processed using diaminobenzidine as chromogen, using a standard ABC kit (Vector Labs, Burlingame, CA). A light cresyl violet Nissl counterstain was used to identify the cortical layers.

Immunofluorescence

Brains for immunohistochemistry were exctracted from three rats previously anesthetized using 30% isofluorane and perfused transcardially with 0.1 M PBS, followed by 4% paraformaldehyde fixative. Once removed from the skull, brains were postfixed overnight at 4°C in the same solution and stored at the same temperature in cryoprotective solution (20% glycerol) until sectioning. Forty-micrometer-thick sections were cut on a microtome (Micron HM 430) and stored at 4°C in 0.1 M PBS with 0.001% NaN_3. Free-floating sections were washed in 0.1 M PBS and incubated for 1 h at room temperature (RT) in blocking buffer [0.1 M PBS, 3% normal goat serum (NGS), and 0.3% Triton X-100]. Primary antibodies were diluted in dilution buffer containing 0.1 M PBS, 2% NGS, and 0.3% Tween-20. Sections were incubated with monoclonal rat anti-M2AchR (1:50; MAB367, Chemicon) and either rabbit anti-parvalbumin (1:6,000; AB9312, Chemicon), mouse anti-somatostatin (1:10; V1169, Biomeda), or rabbit anti-calbindin (1:2,500; AB1778, Chemicon) at 4°C for 48 h on a shaker. After primary incubation, sections were washed 5 times for 10 min with 0.1 M PBS. The sections were incubated for 2 h at RT with the respective secondary antibodies (Cy-5 Goat Anti-Rat and Cy-2 Goat Anti-Rabbit or Cy-2 Goat Anti-Mouse, Jackson ImmunoResearch) diluted 1:200 in 0.1 M PBS. After secondary incubation, sections were washed 5 times for 10 min with 0.1 M PBS and mounted on glass slides with DPX (Fluka 44581) and observed using a confocal microscope.

Statistical analysis

We defined a statistically stable period as a time interval (3–5 min) along which the IPSC mean amplitude measured during any 1-min assessment did not vary according to an unpaired Student's *t*-test. Means ± SE are reported. Pair pulse ratio (PPR) was calculated as the mean of the second response divided by the mean of the first response, according to Kim and Alger (2001).

The effects of drug application on the IPSC amplitude changes are reported as R (reduction) $\equiv 100 \times (1 - A_{treat}/A_{ctrl})$, where A_{treat} and A_{ctrl} were, respectively, the mean IPSC amplitude in treatment or in control ($R = 0$ corresponded to no change, whereas $R = 100$ corresponded to total block). Drug effects were assessed by measuring and comparing the different parameters (R, IPSC mean amplitude, PPR, and others) between baseline (control) versus treatment, with paired Student's *t*-test. ANOVA unpaired Student's *t*-tests were used for comparisons between different groups of cells, and the Wilcoxon test was used for comparing between PPRs. Data were reported as different only if $P < 0.05$%, unless indicated otherwise. Single asterisks (*) indicate $P < 0.05$, double asterisks (**) indicate $P < 0.02$.

Quantal analysis was performed to identify the locus of effect of drugs affecting postsynaptic current amplitudes. We used a CV analysis similar to the one reported by Faber and Korn (1991) and by Zucker and Regehr (2002) to determine the synaptic locus, and by Clements and Silver (2000) to calculate eIPSC quantum amplitude.

RESULTS

Pharmacologically isolated GABAergic currents were measured in neurons voltage-clamped at $V_h = -60$ mV. Input resistance was 219 ± 24 MΩ ($n = 16$). eIPSCs were blocked by bicuculline (10 μM, $n = 6$), indicative of their GABAergic origin (Fig. 1*A*; time-course in Fig. 1*B*). Biocytin staining showed that the majority of the recorded cells were spiny neurons displaying either a stereotypical pyramidal morphology with extensive basal dendrite and an apical dendrite portraying a characteristic fan-like expansion in the superficial layers (Fig. 1*C*) or a more radial symmetric dendritic arborization (Fig. 1*D*).

Effect of oxotremorine on $GABA_A$R-mediated currents

To study the effect of the activation of muscarinic receptors on the inhibitory synaptic signals, we bath-applied the prototypical muscarinic agonists muscarine (1 μM) or oxotremorine (10 μM) after recording a stable baseline response for 7–10 min. We defined the reduction as $R \equiv 100 \times (1 - A_{treat}/A_{ctrl})$ ($R = 100$ equals total block). Application of either drug greatly decreased the mean eIPSC amplitude ($R = 57 \pm 7\%$ decrease in muscarine, 6/7 cells; Fig. 2*A* $R = 69 \pm 7\%$ in oxotremorine, 14/15 cells; Fig. 2*B*) without changing the input resistance >10%. Muscarine and oxotremorine also increased paired pulse ratio (PPR), defined as the ratio between the mean of the second to the mean of the first eIPSCs amplitudes (Kim and Alger 2001) (PPR: 1.01 ± 0.08 in control vs. 1.33 ± 0.06 in muscarine, $n = 6$, $P < 0.02$; Fig. 2*C*; PPR: 0.9 ± 0.06 in control vs. 1.25 ± 0.9 in oxotremorine; Fig. 2*D*; $n = 14$, $P < 0.01$, Wilcoxon′s *t*-test). The eIPSC amplitude decrease was prevented by previous application of the muscarinic blocker atropine (3 μM, $R = 5 \pm 3\%$, $n = 3$; Fig. 2*E*), confirming the muscarinic nature of the depression. Mean values of the synaptic amplitude and PPR are reported in Fig. 2, *F* and *G*.

We did not detect any effect of muscarinic agonists on the eIPSC kinetics (rise-time = 2.2 ± 0.2 ms in control vs. 2.3 ± 0.2 ms in oxotremorine, not significant; decay time was 35 ± 1.5 ms in control vs. 34 ± 2 ms in oxotremorine, not significant).

Synaptic locus of the muscarinic-induced IPSC depression

A decrease in eIPSC amplitude accompanied by an increase in PPR might reflect a change in neurotransmitter release probability (Baldelli et al. 2005). To test the hypoth-

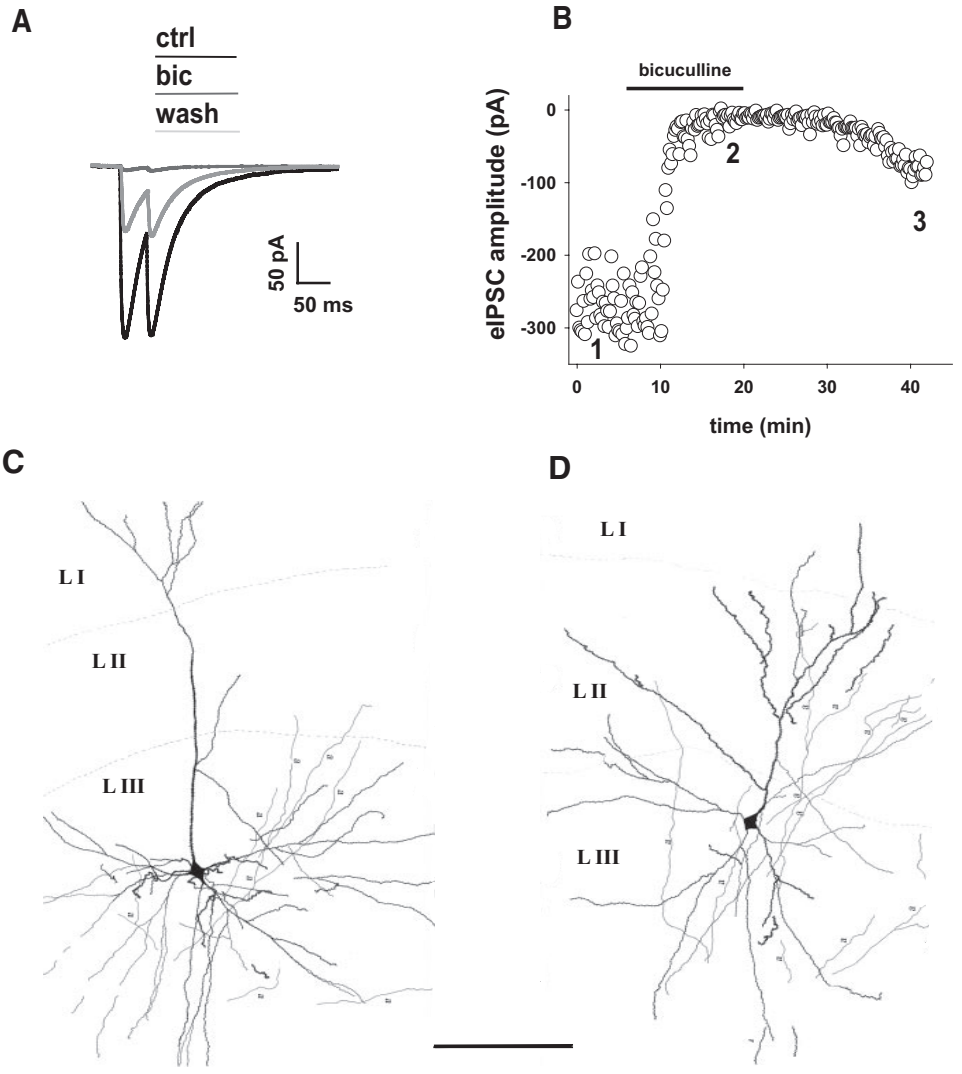

FIG. 1. GABAergic currents in supragranular auditory cortex layers. *A*: synaptic currents were evoked by electrical stimulation at <300 μm from the recording site with a pair pulse protocol (interpulse interval = 50 ms) at holding potential $V_h = -60$ mV in the presence of the glutamate receptor blockers DNQX (10 μM) and kynurenate (2 mM). Traces are averages of 20–30 adjacent traces in control, after bicuculline application, and after bicuculline washout. *B*: time-course of effect of bicuculline. Evoked inhibitory postsynaptic current (eIPSC) amplitude of the 1st response is reported vs. time (stimulation frequency, 0.1 Hz). Responses are reversibly blocked by bicuculline, proving their GABAergic origin. *C*: camera lucida drawing of a typical cortical spiny cell with basal dendrites and neuropil expansion of its apical dendrite. Calibration bar 100 μm. Symbols (a) show label axonal processes. *D*: supragranular cell with more symmetric morphology and radial dendritic arborization.

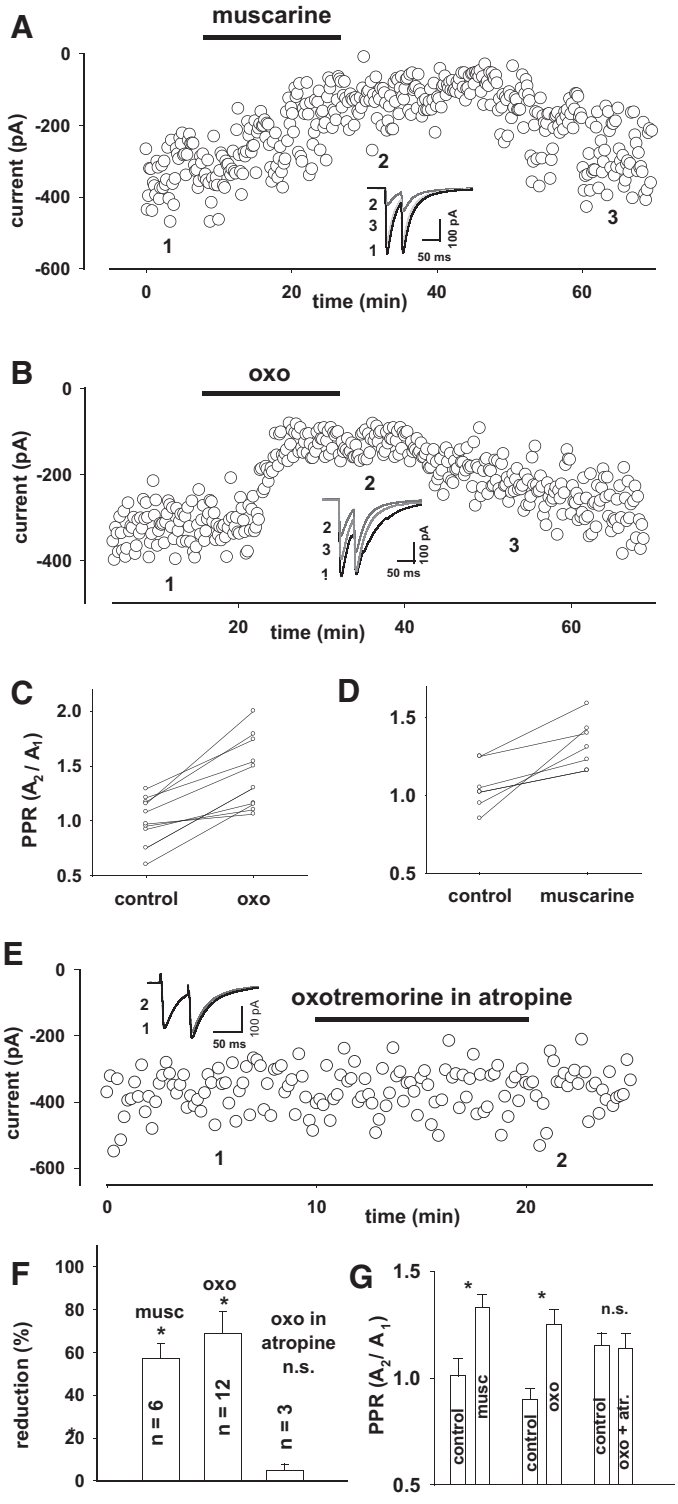

FIG. 2. Activation of muscarinic receptors decreases eIPSC amplitude. *A* and *B*: time-course and traces average (*inset*) of effect of muscarine (1 μM) or oxotremorine (10 μM) on the eIPSC amplitude. Calibration bars: 50 ms, 100 pA. *C* and *D*: changes in pair pulse ratio (PPR) for individual cells after application of oxo or muscarine. *E*: same as *B* but in the presence of the muscarinic antagonist atropine (3 μM). *Inset* calibration bars: 50 ms, 200 pA. *D*: summary of amplitude change in different conditions. *F* and *G*: average amplitude and PPR change induced by muscarine, oxotremorine, and oxotremorine in the presence of atropine. Sample size in *G* is the same as in *F* (in or above bars).

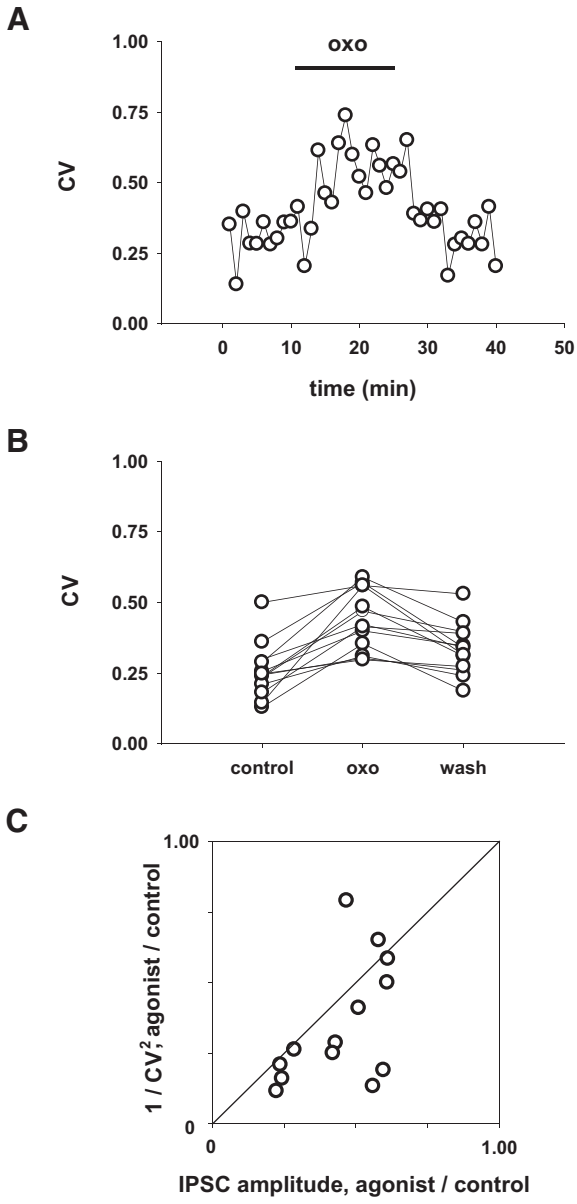

FIG. 3. CV analysis of the muscarinic amplitude decrease. *A*: representative time-course of variation of CV during application of oxotremorine (bar). Every point represents value of CV averaged over a time period of 1 min. *B*: change in CV value in individual recordings in control, during oxotremorine application, and after washout. *C*: CV^2 analysis, every point represents 1 single cell recording; in abscissa is ratio of eIPSC amplitudes after oxotremorine application divided by control amplitude. In ordinate is $1/CV^2$ in oxotremorine divided by $1/CV^2$ in control. Quantal analysis suggests that points below identity are caused by presynaptic effects.

esis of a presynaptic involvement, we systematically performed the analysis of the eIPSC CV, which showed an increase in CV after oxotremorine application (0.23 $\pm$ 0.025 in control vs. 0.47 $\pm$ 0.040 in oxotremorine, $P < 0.0001$, Student *t*-test), as shown in the example in Fig. 3*A*. Similar to the muscarinic amplitude change, the increase in CV (shown in Fig. 3*B* for each individual recording) is in large part reversible. In Fig. 3*C*, CV^2 analysis indicates a presynaptic locus (Faber and Korn 1991). Quantal amplitude (*Q*) derived from quantal analysis (Clements and Silver 2000)

was not changed by oxotremorine ($Q = 10 \pm 1$ pA in control vs. $Q = 11 \pm 2$ pA in oxotremorine, not significant, data not shown).

As a second assay, we used brief pressure applications of the $GABA_A$ agonist muscimol (100 μM) to test the effect of oxotremorine on the chemically evoked postsynaptic currents (cIPSC). cIPSC resulted in prolonged inward currents decaying in several seconds, greatly outlasting drug applications (lasting only a few milliseconds, see METHODS). Oxotremorine failed to alter cIPSC amplitude (representative example in Fig. 4*A*; mean in Fig. 4*B*; $R = -5 \pm 4\%$, $n = 10$, not significant).

We tested the hypothesis that the activation of muscarinic receptors was directly affecting presynaptic release mechanisms. To do so we measured the effect of oxotremorine on the amplitude and frequency of miniature IPSCs (mIPSCs) in the presence of the Na^+-channel blocker TTX (0.5 μM). Neither the frequency nor the amplitude of mIPSC in TTX was altered by application of the muscarinic agonist (representative traces and cumulative histograms of amplitude and frequency are shown in Fig. 4, *C–E*, respectively). Mean eIPSC amplitude was 14.5 ± 0.2 pA in oxotremorine versus 14 ± 0.2 in control (Fig. 4*F*; same sample, not significant). Mean frequency was $f = 1.10 \pm 0.30$ Hz in oxotremorine versus 1.07 ± 0.20 Hz in control (Fig. 4*G*; $n = 11$, not significant).

The invariance of the quantal amplitude, rise- and decay-time, muscimol-evoked currents, and mIPSC amplitudes after oxotremorine application, together with the change in eIPSC PPR, indicated that the eIPSC current depression is not postsynaptic. The failure of oxotremorine to decrease mIPSC frequency indicated that voltage-gated channels involved in the release of GABA at the axon terminal were possible targets of the muscarinic modulation.

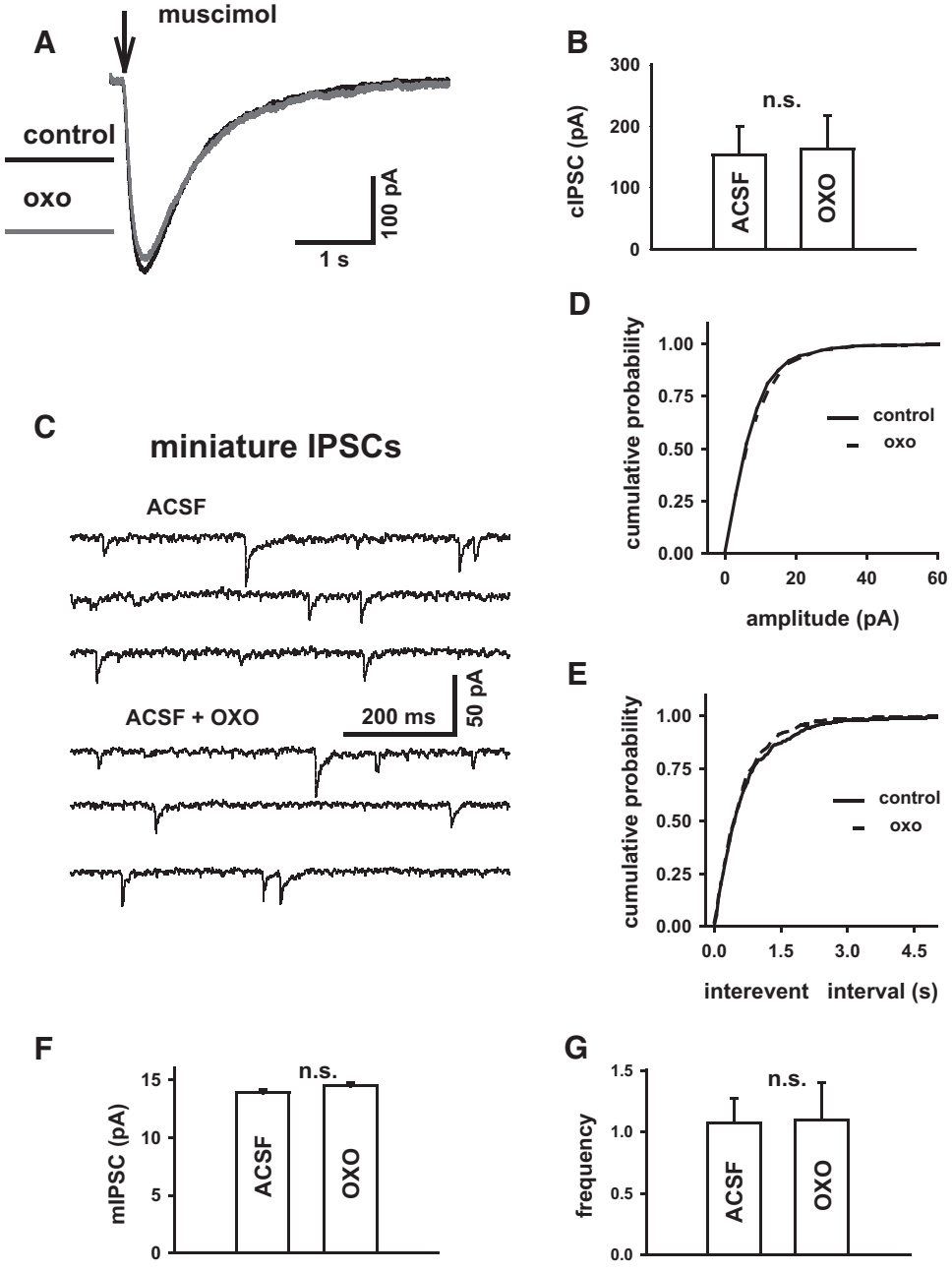

FIG. 4. Synaptic locus of the muscarinic-induced IPSC depression. *A*: 10-ms-long application of the $GABA_A$ agonist muscimol every 30 s reliably evoked an inward current [chemically evoked IPSC (cIPSC)] overlasting stimulus itself (notice the longer time scale). *B*: cIPSC mean amplitude in control or after oxotremorine application ($n = 8$). Bath application of oxotremorine did not alter shape or amplitude of the cIPSC. *C*: representative traces showing that oxotremorine application did not change mean amplitude or frequency of miniature IPSC (mIPSC) in the presence of TTX (0.5 μM). *D* and *E*: cumulative histogram for amplitude and frequency, respectively, are shown for mIPSCs for a representative recording. *F* and *G*: mean of mIPSC amplitude and frequency. Data suggest that a presynaptic but spike-dependent process is responsible for muscarinic depression of eIPSC amplitude.

Calcium channels are the target of muscarinic receptor activation

We tested the possibility that the activation of muscarinic receptors induced the decrease in GABA release by targeting axonal calcium channels by first determining which type of Ca^{2+} channels were responsible for the release of GABA. Application of the selective N-type Ca^{2+} channel blocker ω-conotoxin GVIA (ω-CgTxGVIA, 1 μM) or of the P/Q-type Ca^{2+} channel blocker ω-agatoxin TK (ω-AgaTK, 200 nM) depressed eIPSC amplitude by 44.5 ± 3 (n = 11) and 78.3 ± 7% (n = 8), respectively. Application of either Ca^{2+} channel blocker changed PPR (PPR = 0.99 ± 0.09 in control vs. 1.2 ± 0.07 in ω-CgTx GVIA, $P < 0.03$, Wilcoxon's t-test; PPR = 0.73 ± 0.08 in control vs. 1.1 ± 0.1 in ω-agatoxin TK, $P < 0.02$, Wilcoxon's t-test) confirmed the presynaptic nature of the effect. Examples of time-course and traces are reported in Fig. 5*A* for ω-CgTxGVIA (PPR for each individual cell in Fig. 5*B*) and in Fig. 5*C* for ω-AgaTK (PPR for individual cells in Fig. 5*D*). The mean and PPR for the whole sample is shown in Fig. 5, *E* and *F*, respectively. These results indicate that the relative contribution of P/Q- versus N-type Ca^{2+} channels to GABA release in the cortex is approximately in the ratio 2:1. ω-CgTxGVIA did not affect the eIPSC amplitude in 3/14 recordings, suggestive of an axonal fiber population void of N-type channels.

We next tested the effectiveness of oxotremorine in reducing eIPSC in the presence of ω-CgTxGVIA or ω-AgaTK. In the presence of either toxin, oxotremorine was much less effective in depressing the eIPSC, as shown in the representative time-courses in Fig. 5, *G* and *I*, indicating that both N- and P/Q-type Ca^{2+} channels are involved in the muscarinic-induced depression of the eIPSC amplitude (R = 33 ± 6% in ω-CgTx GVIA, n = 10, $P <$ 0.01, ANOVA with post hoc Tuckey's test; R = 38 ± 3% in ω-Aga Tx TK, n = 7, $P < 0.05$, ANOVA with post hoc Tuckey's test; mean in Fig. 5*K*). Even in the presence of either Ca^{2+} channel blocker, oxotremorine application was still followed by a change in PPR (PPR = 1.2 ± 0.07 in ω-CgTx GVIA alone vs. 1.34 ± 0.08 in ω-CgTx plus oxotremorine, $P < 0.05$ Wilcoxon's t-test; Fig. 5*H*; in presence of ω-Aga Tx TK alone PPR = 1.01 ± 0.1 vs. ω-Aga Tx TK plus oxotremorine, PPR = 1.3 ± 0.1, $P <$ 0.05 Wilcoxon's t-test; Fig. 5*J*), confirming again its presynaptic effect. Summary of the action of oxotremorine in the presence of the Ca^{2+} blockers on PPR is shown in Fig. 5*L*.

Muscarinic receptors responsible for the depression of GABA release

Because activation of muscarinic M_1Rs reduces GABA release in the visual cortex (Kimura and Baughman 1997), we tested the hypothesis that the same receptor type was respon-

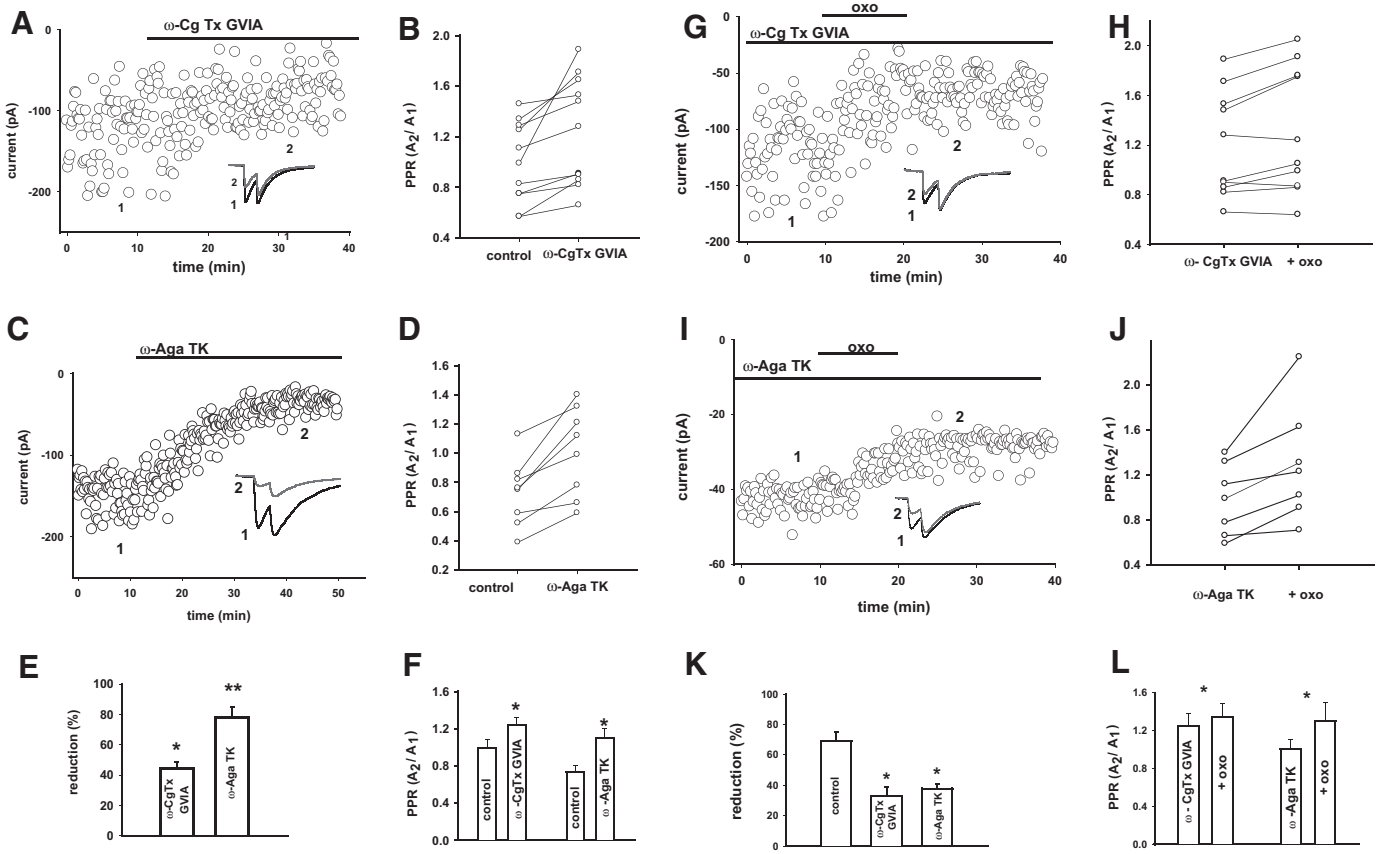

FIG. 5. Ca^{2+} channels are target of the muscarinic depression. N-type and P/Q-type Ca^{2+} channels induce the release of GABA. *A* and *B*: representative time-course (traces in *inset*) and individual changes in PPR after application of the N-type blocker ω-CgTxGVIA (1 μM). *C* and *D*: like *A* and *B*, but after application of ω-AgaTK (200 nM). *E* and *F*: mean ± SE of eIPSC amplitude reduction and PPR after ω-CgTxGVIA or ω-AgaTK (200 nM). *G* and *H*: representative time-course (traces in *inset*) and individual changes in PPR after application of oxotremorine in the presence of ω-CTxGVIA. *I* and *J*: same as in *G* and *J* but after application of ω-Aga TK. *K*: summary of effect of oxotremorine in the presence of ω-CTxGVIA or ω-Aga TK compared with control. Presence of either toxin removed approximately one half of muscarinic reduction of eIPSC amplitude. *L*: mean ± SE of oxotremorine-induced change in PPR in the presence of ω-CTxGVIA or ω-Aga TK.

sible for the depression of the GABA signal in the auditory cortex. To test this hypothesis, we measured the effect of the selective M_1R agonist MT1 (100 nM) on eIPSC amplitude. MT1 decreased eIPSC amplitude albeit to a lesser extent (25 ± 7%; example of time-course in Fig. 6*A*; $n = 8$) with respect to the depression elicited by either oxotremorine ($R = 69\%$) or muscarine ($R = 57\%$, $P < 0.04$, ANOVA with post hoc Tukey's test). Consistently with the latter result, the presence of the specific blocker for M_1Rs MT7 (20 nM) had a statistically significant but modest effect in preventing oxotremorine from decreasing eIPSC amplitude ($R = 44 \pm 3\%$, $n = 7$, $P < 0.03$, ANOVA with post hoc Tukey's test; Fig. 6*B*). On the

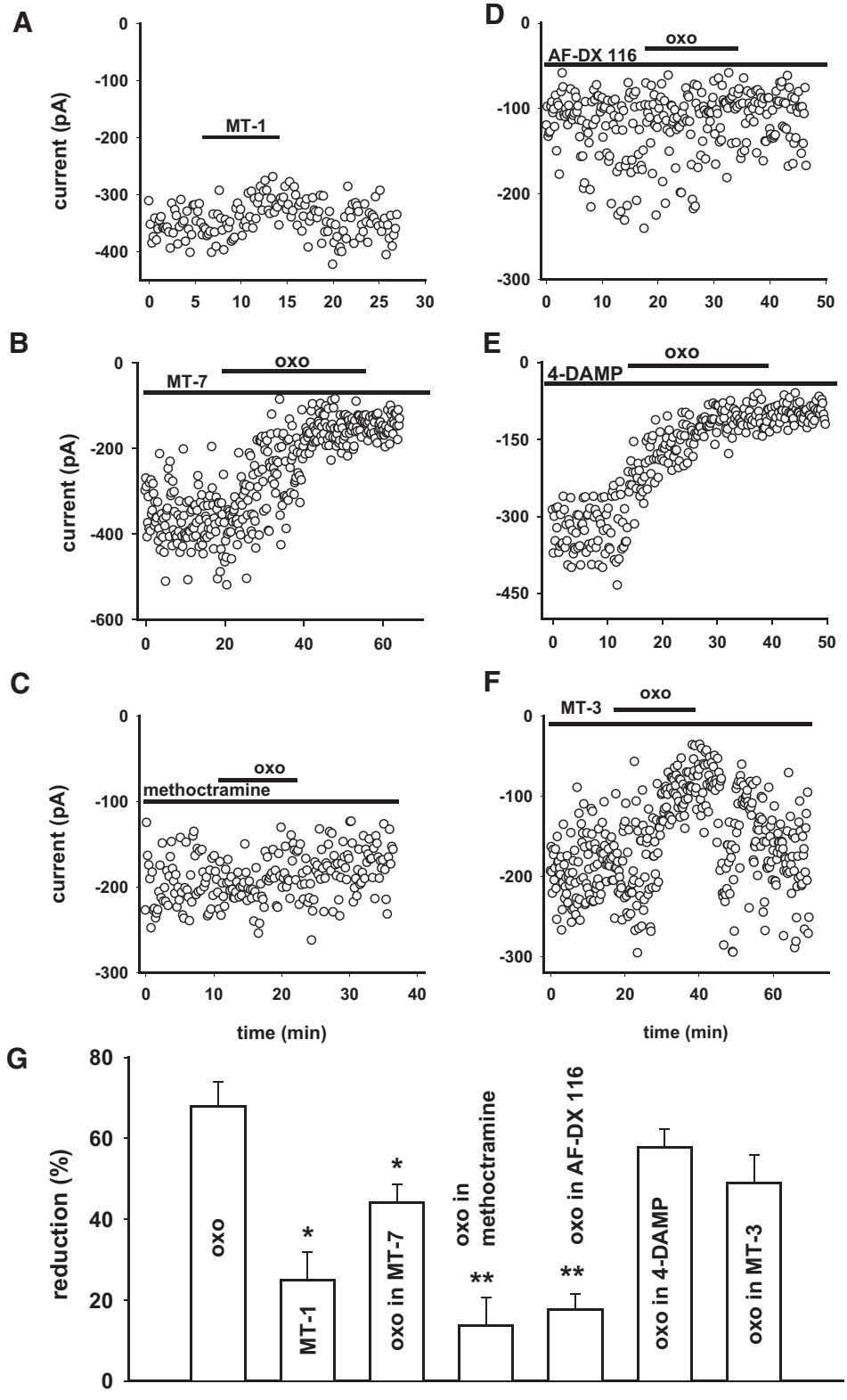

FIG. 6. M_2 receptors (M_2Rs) mediate the muscarinic-induced inhibition of GABA release. Representative time-course of effects of muscarinic receptor agonists and antagonists. *A*: time-course eIPSC depression by the selective M_1R agonist MT1 (100 nM). *B*: presence of specific M_1R blocker MT-7 only slightly decreases the muscarinic depression. *C* and *D*: presence of M_2R antagonists methoctramine or AF-DX 116 blocks the oxotremorine-induced eIPSC reduction, respectively. *E*: M_3R 4-DAMP (100 nM) does not alter the muscarinic eIPSC reduction. *F*: M_4R antagonist MT-3 (50 nM) does not change the oxotremorine-induced eIPSC depression. *G*: summary of results of experiments with muscarinic toxins and antagonists, suggesting that M_2Rs are responsible for muscarinic-induced eIPSC reduction.

contrary, the presence of the M_2R blockers methoctramine (5 μM) or AF-DX 116 (1 μM) successfully prevented eIPSC depression ($R = 14 \pm 5\%$, $n = 7$ and $18 \pm 3\%$, $n = 7$, respectively; Fig. 6, *C* and *D*; $P < 0.01$, ANOVA with post hoc Tukey′s test). The M_4R-blocker MT3 (50 nM) or the M_3R-blocker 4-DAMP (100 nM) failed to block the depressant action of oxotremorine on the eIPSC ($R = 54 \pm 7$ and $58 \pm 4.5\%$, $P > 0.05$ for both, not significant, ANOVA with post hoc Tukey′s test; Fig. 6, *E* and *F*). In summary, as shown in Fig. 6*G,* displaying mean ± SE from the experiments reported above, M_1Rs and M_2Rs seem to be responsible for about one third and two thirds, respectively, of the depression of GABA.

Co-localization of M_2Rs and interneuronal markers

Although the presence of M_1Rs has been documented in both pyramidal cells and GABAergic neurons (Kimura and Baughman 1997; Mash and Potter 1986; Perez-Rosello et al. 2005), the role and localization of cortical M_2Rs has been less studied. For this reason, we studied the possible co-localization of M_2Rs with the interneuronal marker, parvalbumin (PV), calbindin (CB), or somatostatin (SOM). Commercial antibodies were used (see METHODS) to identify the presence of the corresponding antigens with fluorescent methods. We first performed a series of control experiments with *1*) only one primary for the interneuronal marker or M_2Rs + both secondary antibodies, *2*) one primary and the nonmatched secondary antibody, *3*) both secondary but no primary antibodies, or *4*) single labeling either primary + matched secondary. PV- and CB-positive cells were detected in a relatively large neuronal population spanning through the six cortical layers (Fig. 7), including round-shaped cell bodies, whereas the density of SOM-positive cells was much lower than that of PV- or CB-positive cells (~10 times lower, data not shown). M_2R-positive cells were also detected throughout the cortical layers and corresponded to a relatively large neuronal population with either pyramidal-like or round cells bodies. At the dilutions indicated (see METHODS), all control experiments gave results consistent with the specificity of the antibodies. Double labeling experiments in auditory cortex sections from three animals displayed that approximately one half (50.4%) of the PV-positive cells resulted positive for M_2Rs, whereas 92.9% of the CB-positive cells were also M_2R-positive (Fig. 7, *D–F*). SOM-positive cells as well displayed a high degree of co-localization with M_2R-positive cells (70.4%). All these data corroborate our hypothesis that M_2Rs are present in GABAergic neurons.

Both M_1Rs and M_2Rs affect the ω-CgTxGVIA–insensitive component of GABA release

We concluded this series of experiments by determining the contribution of M_1Rs and M_2Rs to the ω-CgTxGVIA–insensitive component of GABA release (presumably P/Q type channel-dependent). We found that, in the presence of ω-CgTxGVIA plus the M_1R antagonist MT7, oxotremorine did not block eIPSCs ($R = 8 \pm 3\%$; representative time-course in Fig. 8*A*), whereas in ω-CgTxGVIA plus the M_2R antagonist AF-DX 116, the block was $R = 23 \pm 3\%$ (representative time-course in Fig. 8*B*), suggesting that, although M_2Rs modulate mainly N-type channels, M_1Rs modulate P/Q-type channels (summary of the mean reduction ±SE in Fig. 8*C*).

PKC and PI_3K mediate most of the muscarinic GABAergic depression

To test whether M_2Rs activated an intracellular second-messenger cascade associated with the $G_{i/o}$-pertussis-sensitive family, we incubated our slices in PTX (50 μg/20 ml), which blocks the effect of $G_{i/o}$ proteins. Although 8- to 12-h slice incubation was not sufficient to prevent muscarinic block ($R = 61 \pm 5\%$, $n = 8$, $P > 0.05$, ANOVA with post hoc Tukey's test), 14- to 18-h incubation did decrease significantly the muscarinic eIPSC reduction ($R = 39 \pm 8\%$, $n = 6$, $P < 0.05$, ANOVA with post hoc Tukey's test). The incomplete block of the muscarinic effect by PTX might be caused by the slow action of the toxin in the tissue.

M_1Rs, M_3Rs, and M_5Rs are supposed to exert their action through PLC. To test whether PLC activation was involved in the muscarinic eIPSC amplitude reduction, we incubated the slices in the presence of the PLC blocker U73122 (10 μM), obtaining only a slight but statistically significant decrease in oxotremorine-induced eIPSC amplitude depression ($R = 43 \pm 3\%$ in U73122, $n = 13$ vs. $69 \pm 6\%$ in control, $P < 0.02$, ANOVA with post hoc Tukey's test; time-course and representative traces in Fig. 9*A*). In the presence of U73122, oxotremorine application still increased PPR (1.60 ± 0.10 in oxotremorine vs. 1.31 ± 0.05 in control, $P < 0.05$). These data suggest that only about one third of the muscarinic modulation was mediated by activation of M_1Rs, indicating that PLC is responsible for only a minor component of the muscarinic-induced eIPSC depression.

We tested the involvement of the PI_3K in the eIPSC depression by incubating slices for 2 h or longer in the presence of a specific blocker of the PI_3K, wortmannin (200 nM) or LY210004 (1 μM). Slice incubation with either blocker almost completely prevented oxotremorine-induced eIPSC amplitude depression ($R = 15 \pm 7\%$ in wortmannin, $n = 8$, $P < 0.01$, ANOVA with post hoc Tukey's test; $R = 20 \pm 3\%$ in LY210004, $n = 6$, $P < 0.01$, ANOVA with post hoc Tukey's test; Fig. 9, *B* and *C*). Application of wortmannin or LY210004 depressed but did not completely prevent the increase in PPR (1.24 ± 0.07 in control vs. 1.42 ± 0.06 in wortmannin, $P < 0.05$; 1.10 ± 0.05 in control vs. 1.23 ± 0.07, $P < 0.05$ in LY210004, $P < 0.05$), suggesting that the nature of the remaining component of the muscarinic depression was still presynaptic.

Because PLC and PI_3K use different types of PKC downhill of their metabolic cascades (Callaghan et al. 2004; Krieg et al. 2002; Oldenburg et al. 2002; Qin et al. 2003), we wanted to study the nature of the possible contribution of different types of PKC in muscarinic eIPSC depression. To do so, we tested the effect of oxotremorine on slices preincubated with either the nonspecific PKC blocker bisindolymaleimide (1 μM) or the specific blocker of the Ca^{2+}-dependent PKC Go6976. Bisindolymaleimide incubation completely blocked the muscarinic effect (Fig. 9*D*; representative time course, $R = 9 \pm 4\%$, $n = 8$, $P < 0.01$, ANOVA with post hoc Tukey's test), whereas Go 6976 preincubation produced results similar to those obtained in the presence of MT-7 and U73122 ($R = 44.5 \pm 2\%$, $P < 0.01$ and $P < 0.05$, ANOVA with post hoc Tukey's test, $n = 7$; Fig. 9*E*), suggesting that Go6976 only occludes the effect produced by M_1Rs. This hypothesis was confirmed by testing the effect of oxotremorine in the presence of Go6976 + the

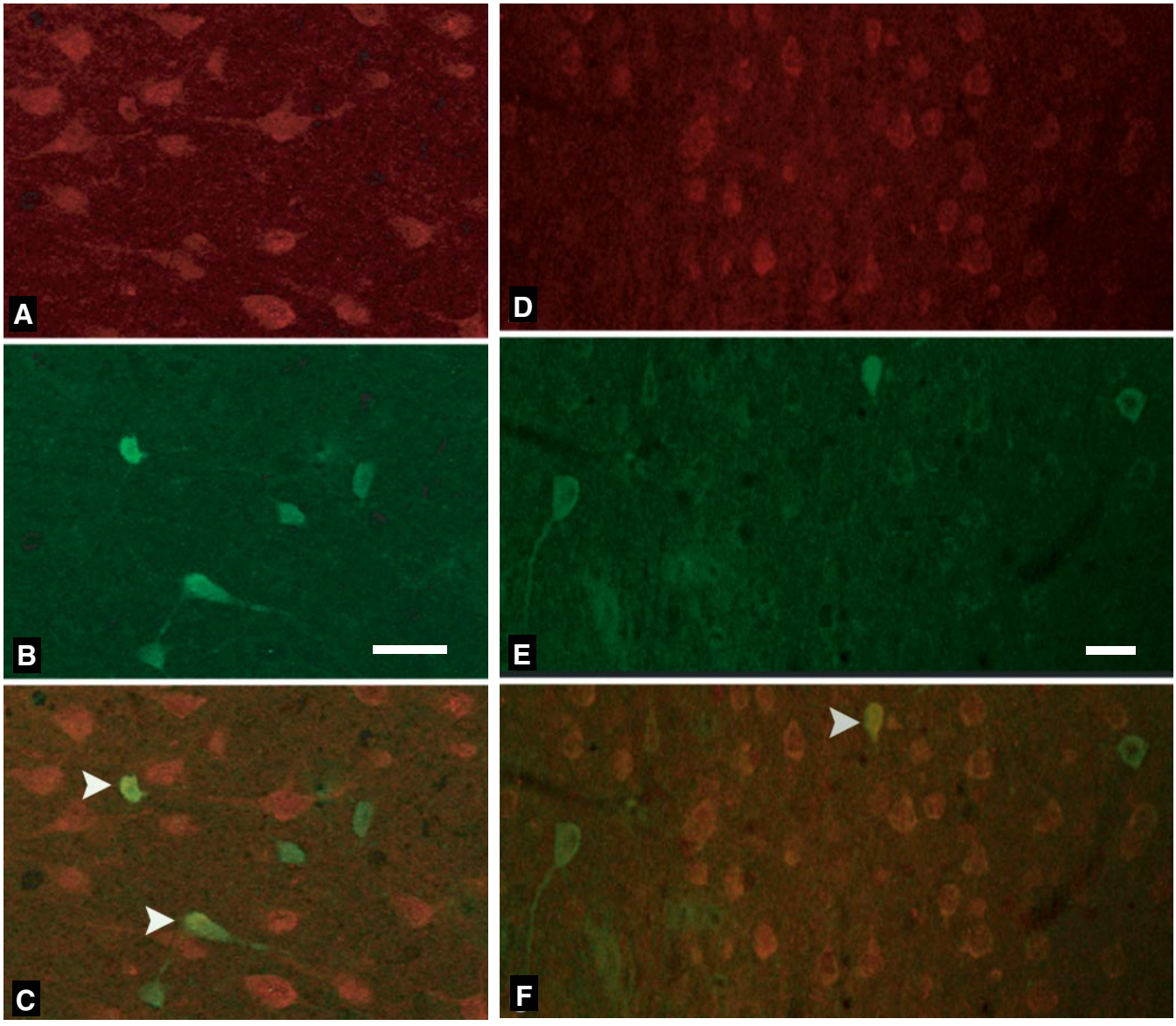

FIG. 7. Muscarinic M_2Rs co-localize with the GABAergic marker parvalbumin (PV). Confocal microscope images of a double-labeling immunofluorescence experiment displaying the co-localization of M_2Rs with interneuronal markers. *A*: Cy5-positive cells in red indicate the presence of M_2Rs. *B*: Cy2-stained cells, in green, are PV-positive. *C*: a subset of PV-positive cells (arrowheads) are also positive to M_2Rs. Co-localization is detected by light yellow. Calibration bar, 20 μm. *D–F*: similar to *A–C*, but with a Cy2-conjugated antibody against calbindin.

M_2R blocker AF-DX 116. The simultaneous presence of Go6976 and AF-DX 116 completely blocked eIPSC depression ($R = 5 \pm 2\%$, $n = 8$, $P < 0.01$, ANOVA with post hoc Tukey's test; Fig. 9*F*). The results are summarized in the bar graph in Fig. 9*G*.

The previous results show that *1*) the whole muscarinic eIPSC depression is PKC-dependent; and *2*) both PKC isoforms, Ca^{2+}-dependent and Ca^{2+}-independent, are responsible for the depression, but M_2Rs only activate the latter one (Ca^{2+}-independent), whereas M1Rs only activate a Ca^{2+}-dependent PKC.

DISCUSSION

Pharmacologically isolated bicuculline-sensitive postsynaptic currents were inhibited in an atropine-sensitive manner by the prototypical muscarinic agonists muscarine and oxotremorine, indicating that GABAergic synaptic currents were blocked by the activation of acetylcholine muscarinic receptors.

Synaptic localization of the muscarinic effect

Several lines of evidence allowed us to trace the synaptic origin of the muscarinic-induced inhibition of GABAergic signal. First, the increase in PPR, CV, and CV^2 analysis, and the invariance in quantal size are all suggestive of a presynaptic origin. Second, mean mIPSCs rise-time, decay-time, and amplitude did not change after oxotremorine application. Third, muscimol-induced currents were also not sensitive to oxotremorine applications. Although we cannot exclude that the GABAergic terminals generating mIPSCs belonged to a dif-

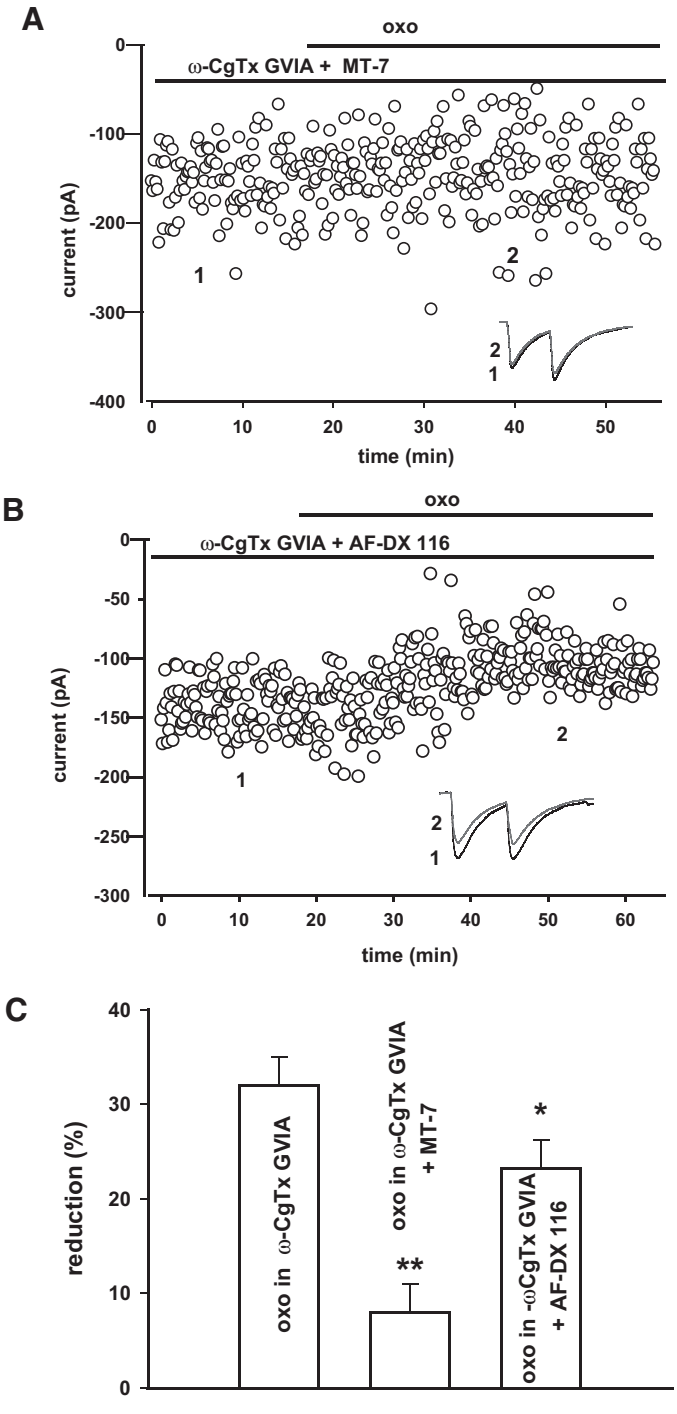

FIG. 8. P/Q channels are modulated by both M_1 and M_2 receptors. Recordings performed in the presence of the N-type Ca^{2+} channel blocker ω-CgTxGVIA (1 μM), leaving intact the P/Q type component of GABA release. *A*: presence of M_1R blocker MT-7 greatly reduces oxotremorine-induced eIPSC depression (time-course, representative traces in *inset*). *B*: presence of M_2R blocker AF-DX 116 reduces only modestly oxotremorine-induced eIPSC depression (representative trace on *right*). *C*: mean ± SE of eIPSC amplitude reduction. Data suggest that P/Q Ca^{2+} channel–related component of GABA release is most sensitive to M_1R and less sensitive to M_2R activation.

ferent class than those generating eIPSCs, these data do not favor the possibility of a postsynaptic locus of action for the muscarinic agonists.

A muscarinic-induced, PKC- and PI_3K-dependent postsynaptic increase in the amplitude of $GABA_A$R-mediated currents has been recently described in the prefrontal cortex (PFC; Ma et al. 2003). The muscarinic-induced change in GABAergic signal in the auditory cortex seems to be caused by mechanisms different from those observed in the PFC. Although we were unable to detect any change in the mIPSCs mean amplitude or frequency or in the response to exogenously applied muscimol, several individual mIPSC recordings displayed an increase in mIPSC amplitude, reminiscent of the effect observed in the PFC (Ma et al. 2003). Regional differences in the composition of $GABA_A$Rs and/or intracellular molecular mechanisms might account for differences between the PFC and the auditory cortex, as we already reported for the muscarinic modulation of glutamate release (Atzori et al. 2005). The insensitivity of mIPSC frequency to oxotremorine suggested a voltage-dependent target in the GABAergic terminal.

Muscarinic receptors modulate N- and P/Q-type calcium channels in GABAergic synaptic terminals

In the mammalian CNS, the N- and P/Q-type channels contribute to synaptic transmission (Arii et al. 1999; Mochida et al. 1998; Sinha et al. 1997; Westenbroek et al. 1998; Wu and Saggau 1997). We examined the role of N- and P/Q-types channels in GABA release in layer II/III of the auditory cortex. Evoked IPSCs were sensitive to both ω-CgTx GVIA and ω-Aga TK, indicating that both N-type and P/Q-type calcium channels are likely to participate in GABA release from auditory cortex terminals. The contribution of P/Q type calcium channels was nearly 80%, whereas the contribution of N-type calcium channels was 45%, suggesting that P/Q type calcium currents, which are the only Ca^{2+}-channels inducing neurotransmitter release in fast-spiking interneurons (Zaitsev et al. 2007), predominantly mediate GABA release in these synapses. The finding that the sum of N- and P/Q-type calcium channels blockade corresponded to >100% inhibition of synaptic transmission is in agreement with previous studies (Lei and McBain 2003; Mintz et al. 1995; Salgado et al. 2005; Wheeler et al. 1996) and is most likely caused by the supralinear relationship between calcium influx and neurotransmitter release (Dodge and Rahamimoff 1967a,b).

The presence of the specific Ca-channel blockers ω-CgTx GVIA or ω-Aga TK greatly impaired the effectiveness of oxotremorine in decreasing eIPSCs amplitude. N-type or P/Q-type Ca^{2+} channel blockers inhibited nearly 50% of the presynaptic inhibition produced by muscarinic receptor activation, suggesting that both N-type and P/Q-type calcium channels are the major (direct or indirect) mediators of the muscarinic eIPSC reduction.

M_2Rs give the largest contribution to the muscarinic GABAergic depression

Different subtypes of muscarinic receptors (M_{1-4}Rs) mediate muscarinic presynaptic inhibition (Fukudome et al. 2004; Li et al. 2004; Perez-Rosello et al. 2005). The recent discovery of toxins acting selectively on different muscarinic receptors [muscarinic toxins (MTs)] (Jerusalinsky and Harvey 1994; Karlsson et al. 2000) helped to dissect the otherwise potentially inaccurate pharmacology of the muscarinic-induced eIPSC

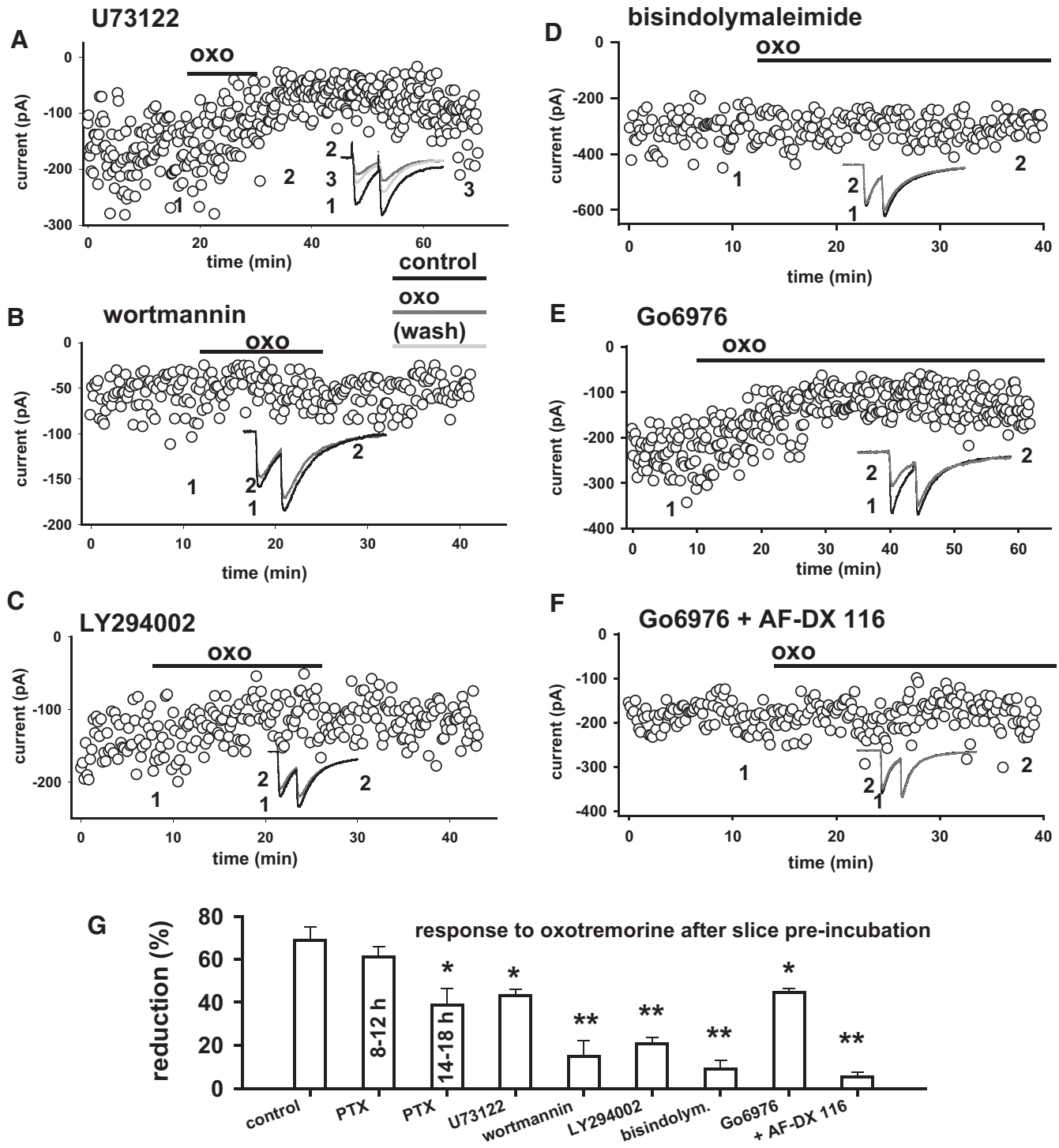

FIG. 9. PI_3K and Ca^{2+}-independent PKC are responsible for most of the muscarinic-induced eIPSC decrease. Effect of slice preincubation with different drugs on the oxotremorine-induced eIPSC modulation. Each letter displays the time-course and representative traces of eIPSC from slices preincubated for ≥2 h with the following: (*A*) PLC blocker U73122 (10 μM), (*B*) PI_3K blockers wortmannin (200 nM), (*C*) LY294002 (1 μM), (*D*) nonspecific PKC blocker bisindolymaleimide (1 μM), (*E*) Go 6976, specific blocker of the Ca^{2+}-dependent PKC, and (*F*) Go 6976 + the M_2R blocker AF-DX 116. *G*: bar graph showing mean ± SE of oxotremorine-induced depression of eIPSC amplitude after slice preincubation with drugs disrupting different intracellular second-messenger pathways. Although 8- to 12-h pertussis toxin (PTX) incubation had no effect, 14- to 18-h incubation did block significantly the muscarinic eIPSC reduction, although to a small degree, possibly because of its slow kinetic action. Similarly, U73122 affected muscarinic eIPSC depression only to a small extent, whereas wortmannin or LY294002 blocked it almost completely. Modest block of the oxotremorine modulation in the presence of U73122 suggests the additional presence of an alternative PLC-independent pathway. The almost complete block of oxotremorine effect by wortmannin or LY294002 indicates a PI_3K involvement in the corresponding second-messenger cascade. The nonspecific PKC blocker bisindolymaleimide completely blocks the oxo-induced eIPSC depression, whereas Go 6976 slightly blocks oxotremorine effect when it acts alone but not in the presence of the M_2R blocker AF-DX 116. Data suggest that M_1Rs and M_2Rs are associated, respectively, with the activation of a Ca^{2+}-dependent and a Ca^{2+}-independent PKC.

decrease. Despite the common tenet that most cortical muscarinic receptors belong to the M_1R or M_4R families, the modest or null effect of the agonist and antagonist of M_1Rs and antagonist of M_4Rs raised the doubt that neither receptor type played a major role in the muscarinic-induced eIPSC decrease. This was confirmed when the presence of either of two specific blockers of M_2Rs completely blocked the muscarinic-induced eIPSC decrease. Co-localization of M_2Rs with the GABAergic interneuronal markers PV, CB, and SOM corroborated further our hypothesis on the role of cortical M_2Rs in GABAergic cells, similar to recent findings in the visual cortex of the monkey (Disney et al. 2006). The extent of the eIPSC depression induced by the specific M_1R agonist and blocked by the M_1R antagonist indicates that the remaining contribution to the muscarinic-induced eIPSC decrease (about one third of the total eIPSC depression) is associated with the activation of M_1Rs.

Several recent studies have shown the presence of M_2Rs in GABAergic interneurons. In particular, two regions adjacent to the temporal cortex, namely the hippocampus and the entorhinal cortex, display co-localization of M_2Rs with the GABAergic interneuronal marker PV in the axon terminals and in the somata (Chaudhuri et al. 2005; Hajos et al. 1998). Our study revealed that one function of M_2Rs in the auditory cortex is the induction of a dramatic decrease of GABA release without directly affecting the interneuronal presynaptic release machinery.

Because the ω-CgTxGVIA–insensitive component of GABA release is presumably represented by P/Q channels, our results suggested that the component of the muscarinic reduction of the GABA release mediated by P/Q of channels is mediated for the most part by M_1Rs located in fast-spiking neurons (Zaitsev et al. 2007) and only modestly by M_2Rs (Fig. 8). A corollary of the preceding results is that, different from P/Q channels, the blockage of the ω-CgTxGVIA–sensitive component of GABA release (N-type channels) is probably mediated completely by activation of M_2Rs.

Metabolic pathway

The great effectiveness of the PKC blocker bisindolymaleimide in preventing the oxotremorine-induced eIPSC block suggested that both M_1R and M_2R modulate GABA release in the auditory cortex by activation of PKC. The involvement of PKC in N- and P/Q-type Ca^{2+} channel modulation has been reported previously by other groups (Perroy et al. 2000; Stefani et al. 2002; Wang et al. 2003). Various isoforms of PKCs are differentially involved in different metabolic pathways and have different sensitivity to Ca^{2+} (Corbalan-Garcia and Gomez-Fernandez 2006). Taking advantage of the existence of a selective drug affecting Ca^{2+}-dependent PKC, we showed that the M_2R-dependent eIPSC depression is mediated by Ca^{2+}-independent PKC, whereas the muscarinic PLC-dependent eIPSC depression seems to be mediated by Ca^{2+}-dependent PKC.

M_2Rs are preferentially coupled to the $G_{i/o}$ protein family, whose activation reduces adenylate cyclase activity and/or inhibits voltage-gated Ca^{2+}-channels (Allen and Brown 1993; Allen et al. 1993; Liu et al. 2003), suggesting a PTX-sensitive mechanism as a possible signaling pathway. On the contrary, the residual M_1R-mediated effect was expected to be preferentially coupled to the hydrolysis of phosphatidylinositol (Exton 1993), similar to the metabolic cascade which depresses the release of glutamate in the same area (Atzori et al. 2005). In agreement with the results obtained with the muscarinic toxins, we found that the inhibition of PLC by U73122 occludes an approximately one-third part of modulation by oxotremorine, confirming that activation of typical PLC-associated M_1Rs is in part responsible for the modulation of GABA release.

The muscarinic eIPSC inhibition was blocked by PTX, as expected for the M_2R-mediated process coupled to G-proteins of the $G_{i/o}$ type (Zhang et al. 2002). The modest reduction by PTX in blocking the muscarinic effect was most likely caused by the incomplete effect of the toxin, whose full extent would require an administration time exceeding the viability of a slice preparation. In smooth myocytes, the activation of muscarinic M_2Rs is coupled to the PI_3K–PKC pathway (Callaghan et al. 2004). The great extent of the block of the muscarinic eIPSC depression after preincubation with different selective PI_3K inhibitors suggests that, also in this case, the PI_3K takes part in the M_2R pathway.

Our experiments did not allow us to determine whether the activation of PI_3K by M_2Rs and that of PKC by PI_3K are direct or indirect or whether or not one type only of GABAergic fibers carried M_1Rs and M_2Rs at the same time, although the absence of eIPSC effect by the N-type channel blocker ω-CgTxGVIA in some recordings suggested the possibility that two population of axonal fibers exist: one void of N-type channels and another containing both N- and P/Q-type Ca^{2+}-channels, similar to a recent finding in the hippocampus (Poncer et al. 2000). Further studies are needed to address this question conclusively.

Functional significance

Several nonmutually exclusive hypotheses could account for a possible physiological significance of the muscarinic-induced decrease in inhibition. One of them could be the promotion of the transition between the sleep and wake states. In fact, the extent of the cholinergic influence in auditory cortical processing depends on the alertness of the animal: during slow-wave sleep, the virtual absence of acetylcholine from the cortex would minimize single cell excitability by allowing a maximal K^+ neuronal conductance (Krnjevic 1993) and maximizing the effectiveness of GABAergic inhibitory currents associated with the thalamic spindles (Lee and McCormick 1997; McCormick 1993; McCormick and Prince 1986). Tonic activation of the corticopetal cholinergic NB produced during the sleep-to-wake transition would produce a basal cholinergic tone activating high-affinity M_2Rs on GABAergic interneurons, inhibiting wave-like release of GABA associated with the sleep state, and increasing the overall responsiveness of the auditory cortex to sensory stimuli.

Another possibility is that the decrease of GABA release after the activation of M_2Rs in GABAergic axons is a phasic function associated with novelty and attention (Sarter et al. 2005a,b). Studies in different sensory cortices report a transient increase in the responsiveness to sensory stimuli associated with the activation of muscarinic receptors. The muscarinic-induced decrease of GABA release might potently increase the excitability of a particular area of the auditory cortex by enhancing its sensitivity to corticopetal thalamic input at the

best frequency in conjunction with nicotinic effects (Hsieh et al. 2000), as well as to cortico-cortical stimuli originating in auditory cortical regions with different best frequencies (Kaur et al. 2005; Metherate et al. 2005).

A third hypothesis, nonmutually exclusive with the previous ones, is that the decrease in glutamate and GABA release associated with the presence of acetylcholine would change the balance between auditory input processed by high-probability synapses versus low-probability synapses, thus favoring a more sophisticated processing of envelope-related information (Atzori et al. 2001). This hypothesis would account for a less effective analysis of auditory information in the case of impaired cholinergic function like Alzheimer disease (Mahendra et al. 2005).

The possibility of the existence of two anatomically and metabolically segregated pathways associated with the decrease of GABA release in functionally different classes of cortical GABAergic interneurons is a hypothesis that needs further exploration. We conclude that the activation of M_2Rs after the activation of cholinergic corticopetal fibers supplies a potent and reversible mean to transiently regulate cortical excitability by decreasing GABA release through the activation of the PI_3K/PKC (Ca^{2+}-independent) metabolic pathway and the activation of M_1Rs through the PLC/PKC (Ca^{2+}-dependent) pathway.

ACKNOWLEDGMENTS

We thank Dr. L. Cauller for support and competent advice throughout this study. H. Salgado determined receptors and metabolic cascades involved in the effect, performed the experiments with all the Ca^{2+} channel blockers and atropine, analyzed them, supplied the material for the figures, and contributed to experimental design and discussion. T. Bellay performed the experiments on oxotremorine decrease of the GABAergic signal, part of the mIPSC recordings, the muscimol pressure application, and the corresponding analysis. J. A. Nichols performed part of the mIPSC and other modulation experiments, analyzed them, and corrected the last version of the manuscript. L. Martinolich and L. Perrotti performed all the immunostaining experiments. M. Bose performed, developed, and analyzed the biocytin-injected fixed samples and their drawings. M. Atzori developed the original idea and wrote the manuscript.

GRANTS

This study was supported by National Institute of Deafness and Other Communication Disorders Grant 1R01-DC-005986-01A1 and National Alliance for Research on Schizophrenia and Depression Foundation/Sidney Baer Trust to M. Atzori and American Academy of Audiology to J. A. Nichols.

REFERENCES

Allen TG, Brown DA. M2 muscarinic receptor-mediated inhibition of the Ca^{2+} current in rat magnocellular cholinergic basal forebrain neurones. *J Physiol* 466: 173–189, 1993.

Allen TG, Sim JA, Brown DA. The whole-cell calcium current in acutely dissociated magnocellular cholinergic basal forebrain neurones of the rat. *J Physiol* 460: 91–116, 1993.

Aramakis VB, Bandrowski AE, Ashe JH. Activation of muscarinic receptors modulates NMDA receptor-mediated responses in auditory cortex. *Exp Brain Res* 113: 484–496, 1997.

Arii T, Ohyanagi M, Shibuya J, Iwasaki T. Increased function of the voltage-dependent calcium channels, without increase of Ca^{2+} release from the sarcoplasmic reticulum in the arterioles of spontaneous hypertensive rats. *Am J Hypertens* 12: 1236–1242, 1999.

Atzori M, Kanold PO, Pineda JC, Flores-Hernandez J, Paz RD. Dopamine prevents muscarinic-induced decrease of glutamate release in the auditory cortex. *Neuroscience* 134: 1153–1165, 2005.

Atzori M, Lei S, Evans DI, Kanold PO, Phillips-Tansey E, McIntyre O, McBain CJ. Differential synaptic processing separates stationary from transient inputs to the auditory cortex. *Nat Neurosci* 4: 1230–1237, 2001.

Baldelli P, Hernandez-Guijo JM, Carabelli V, Carbone E. Brain-derived neurotrophic factor enhances GABA release probability and nonuniform distribution of N- and P/Q-type channels on release sites of hippocampal inhibitory synapses. *J Neurosci* 25: 3358–3368, 2005.

Buhl EH, Tamas G, Fisahn A. Cholinergic activation and tonic excitation induce persistent gamma oscillations in mouse somatosensory cortex in vitro 1. *J Physiol* 513: 117–126, 1998.

Callaghan B, Koh SD, Keef KD. Muscarinic M2 receptor stimulation of Cav1.2b requires phosphatidylinositol 3-kinase, protein kinase C, and c-Src. *Circ Res* 94: 626–633, 2004.

Chaudhuri JD, Hiltunen M, Nykanen M, Yla-Herttuala S, Soininen H, Miettinen R. Localization of M2 muscarinic receptor protein in parvalbumin and calretinin containing cells of the adult rat entorhinal cortex using two complementary methods. *Neuroscience* 131: 557–566, 2005.

Clements JD, Silver RA. Unveiling synaptic plasticity: a new graphical and analytical approach. *Trends Neurosci* 23: 105–113, 2000.

Corbalan-Garcia S, Gomez-Fernandez JC. Protein kinase C regulatory domains: the art of decoding many different signals in membranes. *Biochim Biophys Acta* 1761: 633–654, 2006.

Disney AA, Domakonda KV, Aoki C. Differential expression of muscarinic acetylcholine receptors across excitatory and inhibitory cells in visual cortical areas V1 and V2 of the macaque monkey. *J Comp Neurol* 499: 49–63, 2006.

Dodge FA Jr, Rahamimoff R. Co-operative action a calcium ions in transmitter release at the neuromuscular junction. *J Physiol* 193: 419–432, 1967a.

Dodge FA Jr, Rahamimoff R. On the relationship between calcium concentration and the amplitude of the end-plate potential. *J Physiol* 189: 90P–92P, 1967b.

Exton JH. Role of G proteins in activation of phosphoinositide phospholipase C. *Adv Second Messenger Phosphoprotein Res* 28: 65–72, 1993.

Faber DS, Korn H. Applicability of the coefficient of variation method for analyzing synaptic plasticity. *Biophys J* 60: 1288–1294, 1991.

Fisahn A, Pike FG, Buhl EH, Paulsen O. Cholinergic induction of network oscillations at 40 Hz in the hippocampus in vitro 1. *Nature* 394: 186–189, 1998.

Fukudome Y, Ohno-Shosaku T, Matsui M, Omori Y, Fukaya M, Tsubokawa H, Taketo MM, Watanabe M, Manabe T, Kano M. Two distinct classes of muscarinic action on hippocampal inhibitory synapses: M2-mediated direct suppression and M1/M3-mediated indirect suppression through endocannabinoid signalling. *Eur J Neurosci* 19: 2682–2692, 2004.

Hajos N, Papp EC, Acsady L, Levey AI, Freund TF. Distinct interneuron types express m2 muscarinic receptor immunoreactivity on their dendrites or axon terminals in the hippocampus. *Neuroscience* 82: 355–376, 1998.

Hsieh CY, Cruikshank SJ, Metherate R. Differential modulation of auditory thalamocortical and intracortical synaptic transmission by cholinergic agonist. *Brain Res* 880: 51–64, 2000.

Jerusalinsky D, Harvey AL. Toxins from mamba venoms: small proteins with selectivities for different subtypes of muscarinic acetylcholine receptors. *Trends Pharmacol Sci* 15: 424–430, 1994.

Karlsson E, Jolkkonen M, Mulugeta E, Onali P, Adem A. Snake toxins with high selectivity for subtypes of muscarinic acetylcholine receptors. *Biochimie* 82: 793–806, 2000.

Kaslow HR, Lim LK, Moss J, Lesikar DD. Structure-activity analysis of the activation of pertussis toxin. *Biochemistry* 26: 123–127, 1987.

Kaur S, Rose HJ, Lazar R, Liang K, Metherate R. Spectral integration in primary auditory cortex: laminar processing of afferent input, in vivo and in vitro. *Neuroscience* 134: 1033–1045, 2005.

Kilgard MP, Merzenich MM. Cortical map reorganization enabled by nucleus basalis activity. *Science* 279: 1714–1718, 1998.

Kim J, Alger BE. Random response fluctuations lead to spurious paired-pulse facilitation. *J Neurosci* 21: 9608–9618, 2001.

Kimura F, Baughman RW. Distinct muscarinic receptor subtypes suppress excitatory and inhibitory synaptic responses in cortical neurons. *J Neurophysiol* 77: 709–716, 1997.

Kondo S, Kawaguchi Y. Slow synchronized bursts of inhibitory postsynaptic currents (0.1–0.3 Hz) by cholinergic stimulation in the rat frontal cortex in vitro. *Neuroscience* 107: 551–560, 2001.

Krieg T, Qin Q, McIntosh EC, Cohen MV, Downey JM. ACh and adenosine activate PI3-kinase in rabbit hearts through transactivation of receptor tyrosine kinases. *Am J Physiol Heart Circ Physiol* 283: H2322–H2330, 2002.

Krnjevic K. Central cholinergic mechanisms and function. *Prog Brain Res* 98: 285–292, 1993.

Lee KH, McCormick DA. Modulation of spindle oscillations by acetylcholine, cholecystokinin and 1S,3R-ACPD in the ferret lateral geniculate and perigeniculate nuclei in vitro. *Neuroscience* 77: 335–350, 1997.

Lei S, McBain CJ. GABA B receptor modulation of excitatory and inhibitory synaptic transmission onto rat CA3 hippocampal interneurons. *J Physiol* 546: 439–453, 2003.

Li WC, Soffe SR, Roberts A. Glutamate and acetylcholine corelease at developing synapses. *Proc Natl Acad Sci USA* 101: 15488–15493, 2004.

Liu L, Gonzalez PK, Barrett CF, Rittenhouse AR. The calcium channel ligand FPL 64176 enhances L-type but inhibits N-type neuronal calcium currents. *Neuropharmacology* 45: 281–292, 2003.

Ma XH, Zhong P, Gu Z, Feng J, Yan Z. Muscarinic potentiation of GABA(A) receptor currents is gated by insulin signaling in the prefrontal cortex. *J Neurosci* 23: 1159–1168, 2003.

Mahendra N, Bayles KA, Harris FP. Effect of presentation modality on immediate and delayed recall in individuals with Alzheimer's disease. *Am J Speech Lang Pathol* 14: 144–155, 2005.

Mash DC, Potter LT. Autoradiographic localization of M1 and M2 muscarine receptors in the rat brain. *Neuroscience* 19: 551–564, 1986.

McCormick DA. Actions of acetylcholine in the cerebral cortex and thalamus and implications for function. *Prog Brain Res* 98: 303–308, 1993.

McCormick DA, Prince DA. Acetylcholine induces burst firing in thalamic reticular neurones by activating a potassium conductance. *Nature* 319: 402–405, 1986.

McKenna TM, Ashe JH, Hui GK, Weinberger NM. Muscarinic agonists modulate spontaneous and evoked unit discharge in auditory cortex of cat. *Synapse* 2: 54–68, 1988.

Metherate R, Ashe JH. Basal forebrain stimulation modifies auditory cortex responsiveness by an action at muscarinic receptors. *Brain Res* 559: 163–167, 1991.

Metherate R, Ashe JH. Synaptic interactions involving acetylcholine, glutamate, and GABA in rat auditory cortex. *Exp Brain Res* 107: 59–72, 1995.

Metherate R, Kaur S, Kawai H, Lazar R, Liang K, Rose HJ. Spectral integration in auditory cortex: mechanisms and modulation. *Hear Res* 206: 146–158, 2005.

Mintz IM, Sabatini BL, Regehr WG. Calcium control of transmitter release at a cerebellar synapse. *Neuron* 15: 675–688, 1995.

Mochida S, Yokoyama CT, Kim DK, Itoh K, Catterall WA. Evidence for a voltage-dependent enhancement of neurotransmitter release mediated via the synaptic protein interaction site of N-type Ca^{2+} channels. *Proc Natl Acad Sci USA* 95: 14523–14528, 1998.

Oldenburg O, Qin Q, Sharma AR, Cohen MV, Downey JM, Benoit JN. Acetylcholine leads to free radical production dependent on K(ATP) channels, G(i) proteins, phosphatidylinositol 3-kinase and tyrosine kinase. *Cardiovasc Res* 55: 544–552, 2002.

Passetti F, Dalley JW, O'Connell MT, Everitt BJ, Robbins TW. Increased acetylcholine release in the rat medial prefrontal cortex during performance of a visual attentional task. *Eur J Neurosci* 12: 3051–3058, 2000.

Perez-Rosello T, Figueroa A, Salgado H, Vilchis C, Tecuapetla F, Guzman JN, Galarraga E, Bargas J. Cholinergic control of firing pattern and neurotransmission in rat neostriatal projection neurons: role of CaV2.1 and CaV2.2 Ca^{2+} channels. *J Neurophysiol* 93: 2507–2519, 2005.

Perroy J, Prezeau L, De WM, Shigemoto R, Bockaert J, Fagni L. Selective blockade of P/Q-type calcium channels by the metabotropic glutamate receptor type 7 involves a phospholipase C pathway in neurons. *J Neurosci* 20: 7896–7904, 2000.

Podol'skii II, Vorob'ev VV, Belova NA. Long-term changes in EEG spectra of the hippocampus and neocortex during pharmacological action on the cholinergic system. *Zh Vyssh Nerv Deiat Im I P Pavlova* 50: 982–990, 2000.

Poncer JC, McKinney RA, Gahwiler BH, Thompson SM. Differential control of GABA release at synapses from distinct interneurons in rat hippocampus. *J Physiol* 528: 123–130, 2000.

Qin Q, Downey JM, Cohen MV. Acetylcholine but not adenosine triggers preconditioning through PI3-kinase and a tyrosine kinase. *Am J Physiol Heart Circ Physiol* 284: H727–H734, 2003.

Restuccia D, Della MG, Valeriani M, Rubino M, Paciello N, Vollono C, Capuano A, Tonali P. Influence of cholinergic circuitries in generation of high-frequency somatosensory evoked potentials. *Clin Neurophysiol* 114: 1538–1548, 2003.

Rutkowski RG, Miasnikov AA, Weinberger NM. Characterisation of multiple physiological fields within the anatomical core of rat auditory cortex. *Hear Res* 181: 116–130, 2003.

Salgado H, Tecuapetla F, Perez-Rosello T, Perez-Burgos A, Perez-Garci E, Galarraga E, Bargas J. A reconfiguration of CaV2 Ca^{2+} channel current and its dopaminergic D2 modulation in developing neostriatal neurons. *J Neurophysiol* 94: 3771–3787, 2005.

Sarter M, Hasselmo ME, Bruno JP, Givens B. Unraveling the attentional functions of cortical cholinergic inputs: interactions between signal-driven and cognitive modulation of signal detection. *Brain Res Brain Res Rev* 48: 98–111, 2005a.

Sarter M, Nelson CL, Bruno JP. Cortical cholinergic transmission and cortical information processing in schizophrenia. *Schizophr Bull* 31: 117–138, 2005b.

Sinha SR, Wu LG, Saggau P. Presynaptic calcium dynamics and transmitter release evoked by single action potentials at mammalian central synapses. *Biophys J* 72: 637–651, 1997.

Stefani A, Spadoni F, Martorana A, Lavaroni F, Martella G, Sancesario G, Bernardi G. D2-mediated modulation of N-type calcium currents in rat globus pallidus neurons following dopamine denervation. *Eur J Neurosci* 15: 815–825, 2002.

Voytko ML, Olton DS, Richardson RT, Gorman LK, Tobin JR, Price DL. Basal forebrain lesions in monkeys disrupt attention but not learning and memory. *J Neurosci* 14: 167–186, 1994.

Wang SJ, Su CF, Kuo YH. Fluoxetine depresses glutamate exocytosis in the rat cerebrocortical nerve terminals (synaptosomes) via inhibition of P/Q-type Ca^{2+} channels. *Synapse* 48: 170–177, 2003.

Westenbroek RE, Hoskins L, Catterall WA. Localization of Ca^{2+} channel subtypes on rat spinal motor neurons, interneurons, and nerve terminals. *J Neurosci* 18: 6319–6330, 1998.

Wheeler DB, Randall A, Tsien RW. Changes in action potential duration alter reliance of excitatory synaptic transmission on multiple types of Ca^{2+} channels in rat hippocampus. *J Neurosci* 16: 2226–2237, 1996.

Wu LG, Saggau P. Presynaptic inhibition of elicited neurotransmitter release. *Trends Neurosci* 20: 204–212, 1997.

Xiang Z, Huguenard JR, Prince DA. Cholinergic switching within neocortical inhibitory networks. *Science* 281: 985–988, 1998.

Zaitsev AV, Povysheva NV, Lewis DA, Krimer LS. P/Q-type, but not N-type, calcium channels mediate GABA release from fast-spiking interneurons to pyramidal cells in rat prefrontal cortex. *J Neurophysiol* 97: 3567–3573, 2007.

Zhang Q, Pacheco MA, Doupnik CA. Gating properties of GIRK channels activated by Galpha(o)- and Galpha(i)-coupled muscarinic m2 receptors in Xenopus oocytes: the role of receptor precoupling in RGS modulation. *J Physiol* 545: 355–373, 2002.

Zucker RS, Regehr WG. Short-term synaptic plasticity. *Annu Rev Physiol* 64: 355–405, 2002.